

Microbial biomarkers reveal a hydrothermally active landscape at Olduvai Gorge at the dawn of the Acheulean, 1.7 Ma

Ainara Sistiaga^{a,b,1}, Fatima Husain^a, David Uribebarrea^{c,d}, David M. Martín-Perea^{c,d,e}, Troy Ferland^f, Katherine H. Freeman^f, Fernando Díez-Martín^g, Enrique Baquedano^h, Audax Mabullaⁱ, Manuel Domínguez-Rodrigo^{c,j}, and Roger E. Summons^a

^aDepartment of Earth, Atmospheric and Planetary Sciences, Massachusetts Institute of Technology, Cambridge, MA 02139; ^bGLOBE Institute, University of Copenhagen, 1350 Copenhagen, Denmark; ^cInstitute of Evolution in Africa (IDEA), University of Alcalá, 28010, Madrid, Spain; ^dGeodynamics, Stratigraphy and Palaeontology Department, Complutense University of Madrid, 28040 Madrid, Spain; ^ePaleobiology Department, National Natural Sciences Museum, Consejo Superior de Investigaciones Científicas, 28006 Madrid, Spain; ^fDepartment of Geosciences, The Pennsylvania State University, University Park, PA 16802; ^gDepartment of Prehistory and Archaeology, Universidad de Valladolid, 47002 Valladolid, Spain; ^hRegional Archaeological Museum, 28801 Alcalá de Henares, Spain; ⁱDepartment of Archaeology and Heritage Studies, University of Dar es Salaam, 35050 Dar es Salaam, Tanzania; and ^jDepartment of Philosophy and History (Area of Prehistory), University of Alcalá, 28801 Alcalá de Henares, Spain

Edited by Thure E. Cerling, University of Utah, Salt Lake City, UT, and approved August 14, 2020 (received for review April 10, 2020)

Landscape-scale reconstructions of ancient environments within the cradle of humanity may reveal insights into the relationship between early hominins and the changing resources around them. Many studies of Olduvai Gorge during Pliocene–Pleistocene times have revealed the presence of precession-driven wet–dry cycles atop a general aridification trend, though may underestimate the impact of local-scale conditions on early hominins, who likely experienced a varied and more dynamic landscape. Fossil lipid biomarkers from ancient plants and microbes encode information about their surroundings via their molecular structures and composition, and thus can shed light on past environments. Here, we employ fossil lipid biomarkers to study the paleolandscape at Olduvai Gorge at the emergence of the Acheulean technology, 1.7 Ma, through the Lower Augitic Sandstones layer. In the context of the expansion of savanna grasslands, our results represent a resource-rich mosaic ecosystem populated by groundwater-fed rivers, aquatic plants, angiosperm shrublands, and edible plants. Evidence of a geothermally active landscape is reported via an unusual biomarker distribution consistent with the presence of hydrothermal features seen today at Yellowstone National Park. The study of hydrothermalism in ancient settings and its impact on hominin evolution has not been addressed before, although the association of thermal springs in the proximity of archaeological sites documented here can also be found at other localities. The hydrothermal features and resources present at Olduvai Gorge may have allowed early hominins to thermally process edible plants and meat, supporting the possibility of a prefire stage of human evolution.

biomarkers | thermophiles | hydrothermalism | Olduvai Gorge | paleoenvironment

Olduvai Gorge, located in the Great Rift Valley in Tanzania, has yielded some of the most significant hominin fossils known. The region, notably known because of the work of Mary and Louis Leakey (1), supports active archeological study and archives the emergence of multiple hominin species with diverse stone-tool technologies. However, less is understood about the environments with which early humans may have interacted, though differences in contemporaneous stone tool technologies in the Olduvai region suggest tool specialization. Paleoenvironmental reconstructions of Olduvai Gorge during critical moments in hominin evolution may yield further insight into the history of the human species and may contextualize potential selective pressures in their evolution.

Previous paleoenvironmental reconstructions of Olduvai Gorge focus mainly on Bed I, the oldest deposition layer spanning ~2.1 to 1.78 Ma, and broadly suggest that climate and vegetation at

Olduvai were strongly correlated with precession-driven wet–dry cycles (2–5) imposed upon a general aridification trend (6). The 100,000-y precessional cycles caused the basin vegetation to vary between closed forested ecosystems during wetter periods (2–4, 7) and C4 grass-dominated environments during arid periods. Previous studies also detail the existence of paleolake Olduvai, an alkaline playa (8), phytoliths and plant macrofossils dominated by palms, typha, and sedges (9), diatoms that indicate the presence of paleowetlands (10), and evidence of a tectonically active landscape (11). Oldowan stone-tool technologies used by early hominins, which included scrapers, choppers, and pounders, simple core-flaked tools, have also been recovered from various sites across Bed I (1).

However, less attention has been directed toward Bed II, a younger deposition layer spanning 1.78 to 1.35 Ma, although its geological and stratigraphic history has recently been studied (12). During the deposition of Bed II, the Olduvai region experienced extensive tectonic activity associated with rifting. Tectonic reactivation in the region created a wide graben between the FLK Fault and the Fifth Fault (Fig. 1 *A* and *B*), inducing a several-meter drop in the local base level and the formation of a wide and

Significance

Molecular fossil biomarkers illuminate a geothermally active oasis landscape at Olduvai Gorge 1.7 Ma at the emergence of the Acheulean technology. This study on the local paleolandscape reveals a mosaic ecosystem with great biodiversity, rivers, edible resources, and hydrothermal features. Evidence of hydrothermalism was found near sites intensively used by early hominins. The geothermal activity described here may have influenced the use of the space at Olduvai Gorge and may have provided advantages, such as cooking, which has not been previously contemplated in the context of human evolution.

Author contributions: A.S., D.U., K.H.F., M.D.-R., and R.E.S. designed research; A.S., F.H., and T.F. performed research; A.S., D.M.M.-P., F.D.-M., and M.D.-R. collected samples; D.M.M.-P., F.D.-M., E.B., A.M., and R.E.S. contributed new reagents/analytic tools; A.S., F.H., D.U., K.H.F., M.D.-R., and R.E.S. analyzed data; A.S., F.H., M.D.-R., and R.E.S. wrote the paper; and A.S., D.M.M.-P., F.D.-M., E.B., and A.M. collected samples.

The authors declare no competing interest.

This article is a PNAS Direct Submission.

Published under the PNAS license.

¹To whom correspondence may be addressed. Email: sistiaga@mit.edu.

This article contains supporting information online at <https://www.pnas.org/lookup/suppl/doi:10.1073/pnas.2004532117/-DCSupplemental>.

First published September 15, 2020.

extensive erosive surface throughout the basin, known as the Lower Disconformity (LD), which was infilled within the first half of Bed II by the Lower Augitic Sandstones (LAS) (11). The LAS have been used as a 1.7-My-old chronostratigraphic unit and as an isochronous member that hosts the first appearance of the Acheulean industry at Olduvai Gorge (12, 13). Although the LAS have been considered a unique, complex chronostratigraphic unit in previous works, recent detailed analysis has clarified the presence of two subunits or members: lower and upper. The lower unit is alluvial, very continuous, and covers almost the entire study area. The upper unit is a laterally discontinuous river deposit, which erodes the lower unit in various places, especially in the northwestern half of the study area. Wherever the fluvial erosion is intense, the alluvial lower unit may disappear, and the LAS fluvial upper unit rests directly on the LD.

Bed II contains one of the oldest evidences of the Acheulean technology in the world. The introduction of the technology, which consists of symmetric bifacial stone hand axes, suggests that complex cognition was present 1.7 Ma at Olduvai Gorge. Debates about the emergence, coexistence, and evolution of Acheulean technology have been revitalized by the discovery of FLK West (FLK-W) in Bed II of Olduvai Gorge, located within the LAS layer. This site is contemporaneous with the HWK sites, whose abundant lithic assemblages have been classified as Oldowan (14). The synchronous presence of FLK-W and HWK support the notion that Acheulean and Oldowan technologies coexisted, reinforcing the cladogenetic interpretation of the emergence of the Acheulean and its typological copresence with other industries. The simultaneous presence of Acheulean and Oldowan tools also suggests that both technologies were employed within the same landscape, and that they could have had different uses by early hominins.

Here, we present paleolandscapes reconstructions for the Bed II LAS layer, dated to be 1.7 My-old, which correspond with the appearance of the oldest Acheulean (13, 15, 16) using high-resolution lipid biomarkers and isotopic signatures. Our analysis reveals the presence of a rich mosaic environment different from that of Bed I, with groundwater-fed rivers, aquatic plants, and hydrothermal features, which may have supported remarkable biodiversity in an increasingly arid environment. The hydrothermal activity described may have influenced the use of the space at Olduvai Gorge and may have provided advantages or applied selective pressures not previously contemplated in the context of hominin evolution.

Results and Discussion

Beginning ~3 Ma, pronounced changes in East Africa due to progressive uplift and rifting allowed the gradual replacement of C3 vegetation with C4-dominated grasslands as shown by plant biomarker and isotopic data, marking the beginning of a long-term aridification trend (5, 6, 17). Previous paleoenvironmental reconstructions point to lake expansion–retraction cycles, associated with wetter precession-driven lake refreshing spikes between 1.9 and 1.8 Ma (5, 18), followed by a subsequent major shift toward a drier environment (6, 17). Approximately 1.7 Ma, despite the overarching drying trend, tectonic activity enabled a general reactivation of the drainage network and a progradation of the river systems at Olduvai Gorge.

Plant biomarkers, especially epicuticular leaf waxes, have been widely used to reconstruct paleoclimate and paleovegetation changes in ancient environments, although the chemotaxonomic significance of *n*-alkanes has shown to be intricate (19, 20). All LAS samples analyzed yielded significant amounts of *n*-alkanes. Most of the samples present a distribution dominated by the long-chain, odd-numbered C₂₉, C₃₁, and C₃₃ *n*-alkanes typical of terrigenous inputs (21), while the midchain-length C₂₃ and C₂₅ *n*-alkanes, which have been attributed to the presence of aquatic macrophytes, are also present in significant abundance (22, 23). The *n*-alkane profiles observed here are consistent with a mosaic

ecosystem with contributions from savanna angiosperms, C4 graminoids, and aquatic macrophytes (SI Appendix, Figs. S1 and S2) (19, 20). Notably, LAS 15 shows a high contribution of C₂₃, which has been attributed to *Sphagnum* (24, 25) (SI Appendix, Fig. S1). However, the enriched $\delta^{13}\text{C}_{25}$ values, high ratios of algal lipids relative to algal and terrestrial plant lipids (P_{alg}) (SI Appendix, Fig. S3B and Table S1), and lack of alkan-2-ones, a biomarker for *Sphagnum*, in sample 15 suggest a macrophyte origin instead of Sphagnales (20, 24, 25).

While aquatic macrophytes currently thrive in most high-altitude African lakes, their historical presence at the Olduvai Gorge paleolake was initially confirmed in Bed I (23). The biomolecular proxy P_{aq} (ratios of macrophytic lipids relative to macrophytic and terrestrial lipids) expresses the proportion of submerged and floating macrophytes versus emergent macrophytes and terrestrial plants (22). Most LAS samples have P_{aq} values between 0.2 and 0.4 (Fig. 2B), which correspond to the values suggested for emergent macrophytes, such as plants from the genus *Typha*, fossil imprints for which have been found at Olduvai Gorge within Lower Bed II (26). P_{aq} values below 0.1 are indicative of greater proportions of terrestrial input, confirming that the LAS environments sampled are dominated by emergent aquatic plants, similar to the wetlands present today in Africa (22). Intermediate values between 0.1 and 0.4 reflect a mixed input, pointing to a setting similar to that described for Lake Rutundu in Kenya (22) or Rwenzori National Park in Uganda. Here, abundant floating aquatic plants such as *Potamogeton* in shallow waters with a fringe of emergent macrophytes are surrounded by ericaceous shrubland.

Only LAS 5 had a P_{aq} value above 0.4 ($P_{\text{aq}} = 0.56$), which is consistent with a floating/submerged macrophyte signal. LAS 6 from the HWK-NE archaeological site produced the lowest P_{aq} value of 0.16, which is very close to the terrestrial plant threshold (>0.1), suggesting an increased terrestrial input in this area. Similarly, the terrigenous-to-aquatic fatty acid ratio (SI Appendix, Fig. S3E and Table S1), which reflects the proportion of terrestrial to aquatic sources (33), shows more elevated values for both LAS 6 and LAS 15, which suggests increased terrestrial plant inputs in both HWK-NE and FLK-W. Accordingly, total organic carbon (TOC) values were low in most LAS samples, with nitrogen levels below detection limits (SI Appendix, Fig. S3D).

$\delta^{13}\text{C}$ values for the *n*-alkanes might provide more accurate information concerning the dominant vegetation than $\delta^{13}\text{C}_{\text{TOC}}$, which can carry signals from older, recalcitrant carbon phases. LAS samples have $\delta^{13}\text{C}_{31}$ values that fall within the wooded grassland ecosystem of African plant communities defined by the United Nations Educational, Scientific and Cultural Organization (Fig. 2A). While some samples have C-isotope values approaching those typical of C4 grasses, most $\delta^{13}\text{C}_{31}$ values from LAS samples are within the suggested range for C3 graminoids (2, 3, 20, 21), but they may also point to the presence of aquatic macrophytes, which mostly use the C3 photosynthetic pathway (22, 34). Emergent plants from the genera *Potamogeton*, *Typha*, *Cyperus*, and *Hydrilla* are often predominant in East African wetlands and may display a similar range of $\delta^{13}\text{C}_{25}$ values (SI Appendix, Fig. S3B) (22, 24, 35). However, it is particularly difficult to identify specific taxa given the wide range of $\delta^{13}\text{C}$ values for aquatic plants, which often depend on the differences in isotopic compositions of the source of carbon, water flow, turbulence, and individual physiological properties, such as the relative distribution of the plant above and below the water since this affects the plant's access to HCO_3^- or CO_2 (20, 36). Overall, our biomarker proxies point to a freshwater-fed wetland dominated by C3-graminoids/aquatic macrophytes and woody angiosperms, with a high proportion of aquatic organic matter. This would be in accordance with previous geological and sedimentological descriptions that suggested a marshland dominated by a braided/river environment (11–13).

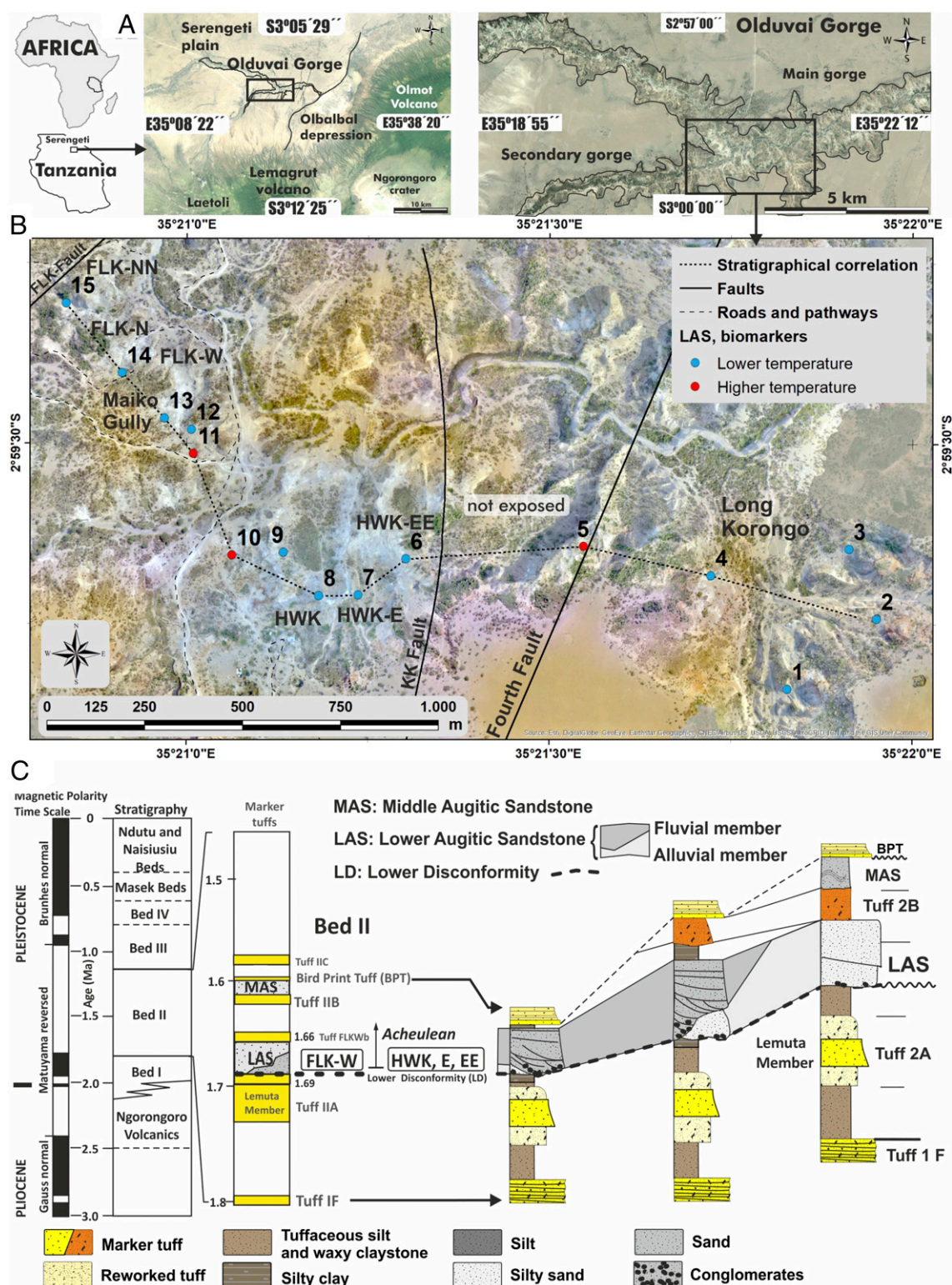


Fig. 1. Study area and sample location. (A) Geographical location of Olduvai Gorge and the study area. (B) Detailed map of the study area, based on the orthoimage obtained with unmanned aerial vehicle. Blue and red dots indicate the position of the samples described in this study. The red color indicates the presence of biomarkers indicative of high-temperature hydrothermal activity. (C) General stratigraphy of Olduvai and synthetic sections of LAS in the study area.

The proportion of C_{28} and C_{29} stanols compared to their sterol homologs has been suggested to be controlled by water levels in peats and thus has potential as a redox biomarker, especially when combined with other proxies such as the humification index

or the concentration of archaeol (diphylanylglycerol) (24). Our C_{29} stanol-to-sterol ratio profile shows values ranging from 0 to 1, average values closer to 1 suggest more reducing depositional conditions (Fig. 2C) (25). Increases seem to be encompassed

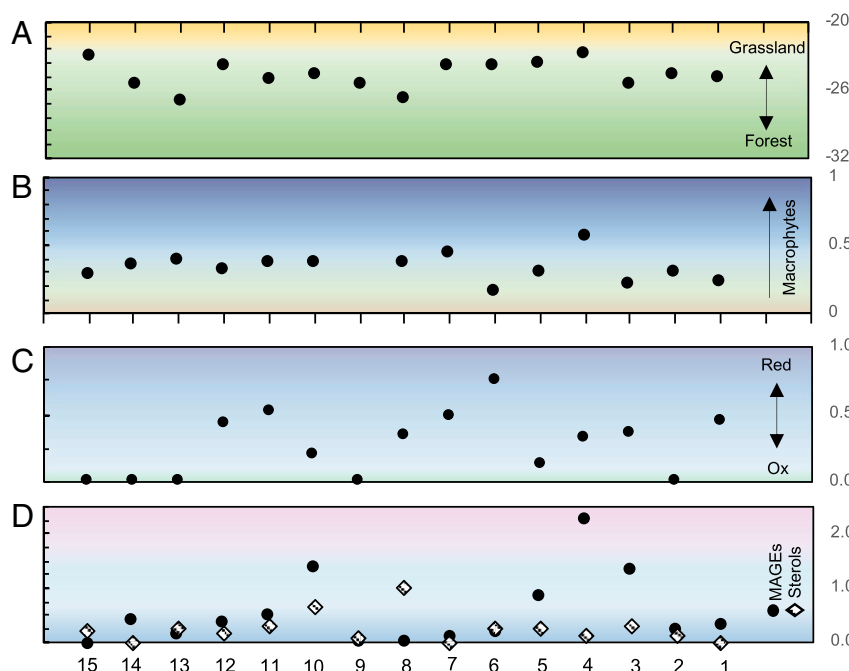


Fig. 2. Geochemical proxies. Plot of various organic geochemical proxies for organic matter preserved in outcrops from eastern fluvial lacustrine deposits (eastern lake margin) dated up to 1.7 Ma at Olduvai Gorge (with descriptive colors). (A) Plant lipid $\delta^{13}\text{C}$ values for $n\text{-C}_{31}$ alkane (higher values indicate more C_4 vegetation) (color gradient denotes drier [yellow] to wetter [green] conditions). (B) Ratios of macrophytic lipids ($n\text{-C}_{23} + n\text{-C}_{25}$) relative to macrophytic and terrestrial lipids ($n\text{-C}_{23} + n\text{-C}_{25} + n\text{-C}_{29} + n\text{-C}_{31}$) (<0.4 = no macrophytes; 0.4 to 1 = emergent macrophytes; >1 = floating macrophytes); color gradient denotes macrophyte input (22). (C) Ratios of C_{29} stanol/ Δ^5 sterol [stigmastanol/(stigmastanol + sitosterol)] (higher values indicative of more reducing conditions); color gradient denotes more oxidizing [green] to more reducing [blue] (24). (D) Abundance of MAGEs and sterols (micrograms per gram of rock) indicating the predominance of MAGEs in some of the LAS samples (color gradient denotes abundance of MAGEs [pink], potentially indicating the a greater contribution from thermophilic microbial communities) (27–32).

with the appearance of archaeol, a marker for anaerobic methanogens, in accord with the anoxic conditions suggested by the ratio. Water levels could be the primary control on archaeol concentrations except for sample 7, which shows an abnormal increase independent of the stanol/sterol ratio.

The analysis of the polar lipid fraction in our samples sheds further light on paleoenvironmental conditions. Samples collected from the LAS layer show a very unusual distribution of functionalized lipids, including monoalkyl glycerol monoethers (MAGEs), which have been often interpreted as biomarkers for sulfate-reducing bacteria (SRB) and/or thermophilic organisms (27, 28, 37), among other possible biological sources (38, 39). These glycerol ether lipids are sometimes present in high concentrations at marine hydrothermal vents and cold seeps and in terrestrial geothermal sediments (27–30). These compounds are structurally stable and might represent the diagenetic products of mixed glycerol ester/ether mixed lipids present in the aforementioned microbial communities. MAGEs are the predominant compound class in our alcohol fraction, constituting more than 80% in some of the samples (Figs. 2D and 3A and B and *SI Appendix*, Tables S3 and S4). Although the source of these molecules is still unclear, such concentrations of MAGEs have mostly been observed in hydrothermal settings (27, 29). A suite of MAGEs ranging from C_{15} to C_{20} with straight, branched, and unsaturated hydrocarbon chains is dominated by the $n\text{-C}_{16}$ MAGE followed by $me\text{-C}_{17:0}$ (*SI Appendix*, Fig. S4), which has been linked in the past to the activity of SRB, more specifically from the genus *Desulphobacter* or *Actinomyces* (39).

MAGEs identified in soils from non-SRB origin are often dominated by $i\text{-C}_{15}$ and $n\text{-C}_{15}$ (39, 40), which are present in very low concentrations in our samples. Although our samples were mostly dominated by $n\text{-C}_{16:0}$ and $me\text{-C}_{17:0}$, LAS 1, 3–4, 8–9, 11,

and 13–14 samples contained significant amounts of MAGEs with a carbon chain length >17 . Longer chain lengths, especially $\text{C}_{18:0}$ and $\text{C}_{20:0}$, have been associated with thermophilic bacteria within the Aquificales (28). In particular, Jahnke et al. (28) found that among the Aquificales bacteria, *Thermocrinis ruber* had a very distinctive lipid signature dominated by C_{18} MAGEs along with large amounts of $\text{C}_{20:1}$, $\text{C}_{22:1}$, and a C_{21} cyclopropane fatty acid ($cy\text{-C}_{21}$) and where glycerol dialkyl ethers were subordinate. Strikingly, none of our samples yielded detectable glycerol dialkyl ethers, which are otherwise common in lake sediments, soils, and marine sediments. LAS 1–3, 5, 8, and 11–14 all contained the $\text{C}_{20:1}$, $\text{C}_{22:1}$ fatty acids, which together with $cy\text{-C}_{21}$ are the dominant fatty acids in *T. ruber* (28). Further, $cy\text{-C}_{21}$ was also identified in samples 5 and 11 (Fig. 4 and *SI Appendix*, Table S2). *T. ruber* is a gram-negative hyperthermophilic bacterium that forms a separate lineage within the Aquificales (28) and was identified for the first time in streamer biofilm communities in Yellowstone hot spring outflow channels (41). *T. ruber* grows optimally between 85°C and 95°C in waters with low salinity and near-neutral pH. *T. ruber* is typically autotrophic and has the ability to oxidize hydrogen, sulfur, and thiosulfate in the presence of oxygen, much like the previously identified thermophilic bacteria *Aquifex* and *Hydrogenobacter* (42). Lipid distributions similar to the ones identified within the LAS samples have been reported in few settings other than the Lower Geyser Basin of Yellowstone National Park, typified by the streamer biofilm communities of features such as Octopus Spring and Bison Pool (Fig. 4) (28, 29, 31), and Orakei Korako Spring (27) in New Zealand. The water chemistry of Aquificales habitats suggest that, apart from temperature, these waters could have been potable, which would have been essential for early humans (10) and animals, considering the salinity of Olduvai Lake (5).

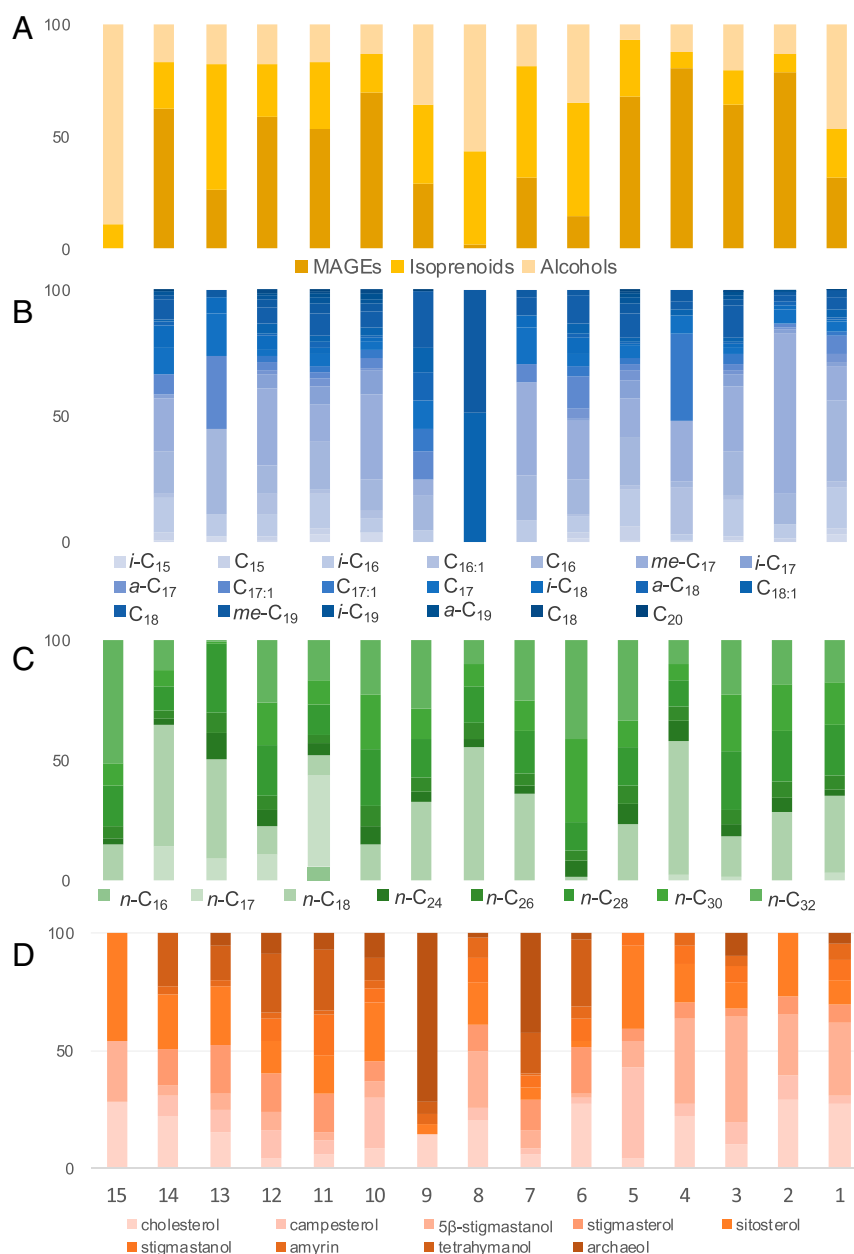


Fig. 3. Polar lipid distributions. Histograms depicting the lipids identified in the GC-MS analysis of the polar fraction. Percentage distributions of (A) distribution of MAGEs, isoprenoids, and *n*-alkanols within each sample, (B) monoalkyl glycerol monoethers, (C) *n*-alkanols, and (D) isoprenoids.

Additional support for the presence of hyperthermophilic microbes comes from the *n*-alkanols and fatty acids, which are dominated by the C_{18} chain length in most of the samples, which, again, has been also identified as a major component in other thermophilic communities (27–29). *n*-Alkanols and fatty acids with longer chains (C_{24} to C_{30}) likely originate from both microbes and detrital plant organic matter (Fig. 3C and *SI Appendix*, Fig. S2 and Tables S2 and S4).

Polyisoprenoid lipids identified in our study include cholesterol, typically derived from animals, the phytosterols sitosterol, stigmasterol, campesterol, and stigmasterol, as well as amyirin, a plant triterpenoid (Fig. 3D and *SI Appendix*, Table S4). Interestingly, some samples contained 5 β -stigmasterol, a biomarker commonly found in herbivore feces (43). LAS 7 and 9 also showed an isoprenoid profile dominated by archaeol, a methanogen biomarker (44). LAS 5, 7, 10, and 11–14 also yielded a polycyclic triterpenoid,

tetrahymanol, which is typically produced by ciliates and also by a few bacteria (45) (*SI Appendix*, Fig. S5) and has also been identified in hydrothermal settings (32). Only a subset of methanotrophs and SRB appear to be able to synthesize tetrahymanol (45), depending on the redox potential of the ecosystem. Tetrahymanol-producing aerobic methanotrophs are often identified in the suboxic zone of marine or freshwater bodies, while SRB occurs in anoxic sediments.

The presence of hydrothermal waters is also supported by the bell-shaped pattern of short chain *n*-alkanes (C_{17} to C_{23}), which can be explained by in situ maturation of organic matter near the hot springs or extrusion of mature sediments with hot fluids, which might have led to the formation of hydrothermal petroleum (46). Mixtures of organic matter from multiple sources may also explain the differences between the $\delta^{13}C_{TOC}$ and the $\delta^{13}C_{31}$ values.

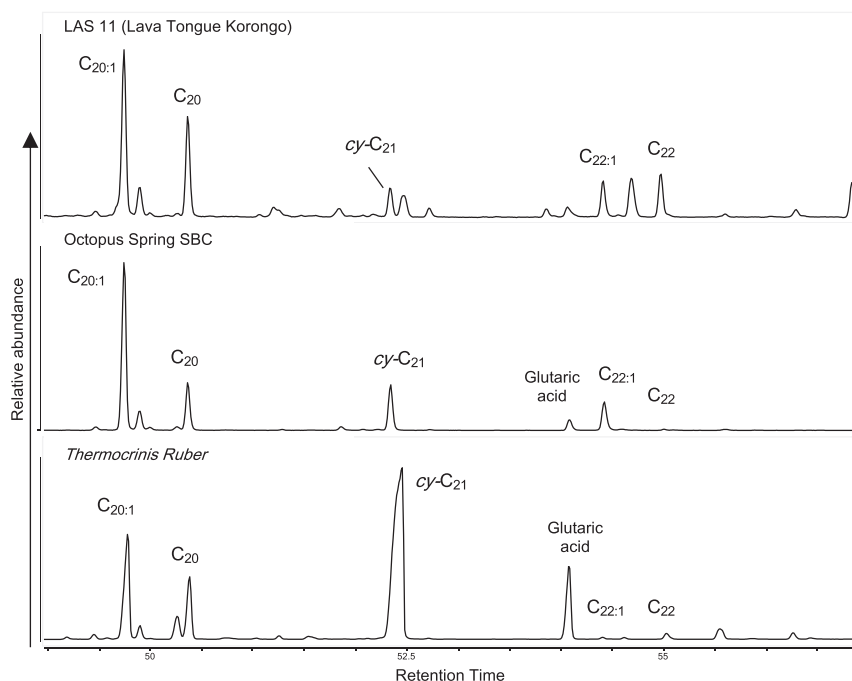


Fig. 4. Comparison of fatty acid distributions in LAS 11, an Octopus Spring streamer biofilm community, and a *T. ruber* culture. (Top) Partial mass chromatogram of fatty acids methyl esters (FAMES) showing the presence of $C_{20:1}$, $C_{22:1}$ and $cy-C_{21}$ extracted from the FAMES of LAS 11. (Middle) Methylated total lipid extract from an Octopus Spring, Yellowstone National Park, streamer biofilm community (28, 29). (Bottom) Methylated total lipid extract from a cultured sample of *T. ruber*.

Most of the LAS samples show coexistence of an early thermally mature component with a fresh and immature fraction (Fig. 5B). A similar phenomenon has been observed at the Pleistocene cherts from Lake Magadi, Kenya, where the biomarker profile showing a co-occurrence of fresh and mature organic matter, MAGEs, tetrahymanol, and alkanols has been interpreted as the result of the presence of a hydrothermal setting (47).

Other microbial lipids were also identified in the LAS samples. LAS 10–12 yielded significant amounts of fern-7-ene and fern-8-ene, which have been attributed to ferns but which are more likely microbial in origin (21). Similarly, hop-17(21)-ene and hop-22(29)-ene are bacterial lipids (21) that were identified in some of the samples.

LAS Landscape and Hominin Evolution

Although the geothermal nature of Olduvai basin has not previously been studied in detail, the presence of hydrothermal systems within the Tanzanian portion of the East African Rift is consistent with conditions exhibited today. Nearby areas such as Lake Natron, Lake Manyara, Lake Eyasi, and Ngorongoro Caldera currently exhibit hydrothermal activity (33, 44). The deposition of the LAS sediments corresponds to an event with major fault activation, that, for the first time, enabled the reactivation and progradation of drainage networks to the Olduvai Basin, changing the nature of the sedimentation from lacustrine to alluvial and fluvial (15). Rift system faults are linked with deep-seated springs, characterized by the temperature and salinity of the water. Contemporary volcanism is characterized by the deposition of rich phenelinites–foidite tuffs and volcanic ashes whose residues can be identified in the LAS sediments. The presence of hydrothermal waters does not appear exclusive to the LAS deposition event, and although no thermal biomolecular markers have been yet found in Bed I, diatom species specifically adapted to warm and hot waters (41), as well as illite/smectite layers potentially suggesting hydrothermalism (48), have

been previously identified in the sequence. The ubiquitous presence of silicified plants (26) is also suggestive of hydrothermal activity.

Our biomarker evidence for distinctive microbial communities (SI Appendix, Fig. S2) points to a paleolandscape influenced by tectonics, volcanism, and hydrothermal activity which will have had implications for early humans at Olduvai Gorge. Bailey et al. (49) earlier suggested that tectonics and volcanism may have created advantages for hominin survival by creating dynamic landscapes that offered protection and resources. The particular tectonic landscape at Olduvai Gorge, fringed by major faults, offered a continuous supply of potable water from rivers and hot springs that would have attracted populations of large herbivores as attested by the fauna recovered in the archaeological sites and paleontological localities contained within LAS (16). The identification of 5 β -stigmastanol in some of our samples, especially upstream and FLK-W, suggests input from terrestrial and aquatic herbivore feces in these samples. Animals could have consumed the waters at Olduvai Gorge much as they do today in Yellowstone National Park, which provided hominins a chance to hunt large prey in a location where the presence of game would be predictable.

At FLK-W sites and its surroundings, proxies such as the stanol to sterol ratio and archaeol, together with the high P_{aq} and P_{alg} (SI Appendix, Table S1), suggest an intermittently waterlogged environment consistent with the wide watercourse previously described (12, 13). This fluvial environment must have been seasonal because the area contains the highest density of stone tool artifacts documented on any Olduvai paleolandscape to date. It also contains a notable density of faunal remains, some of which are in the form of partial carcasses, which suggest the area must have been either a predation arena or a locus of natural death. The intense use of the area by local fauna is additionally supported by the presence of fecal biomarkers. Phytolith evidence from FLK-W points to the presence of grasses and palms (50), consistent with predominance of the C_{31} *n*-alkane

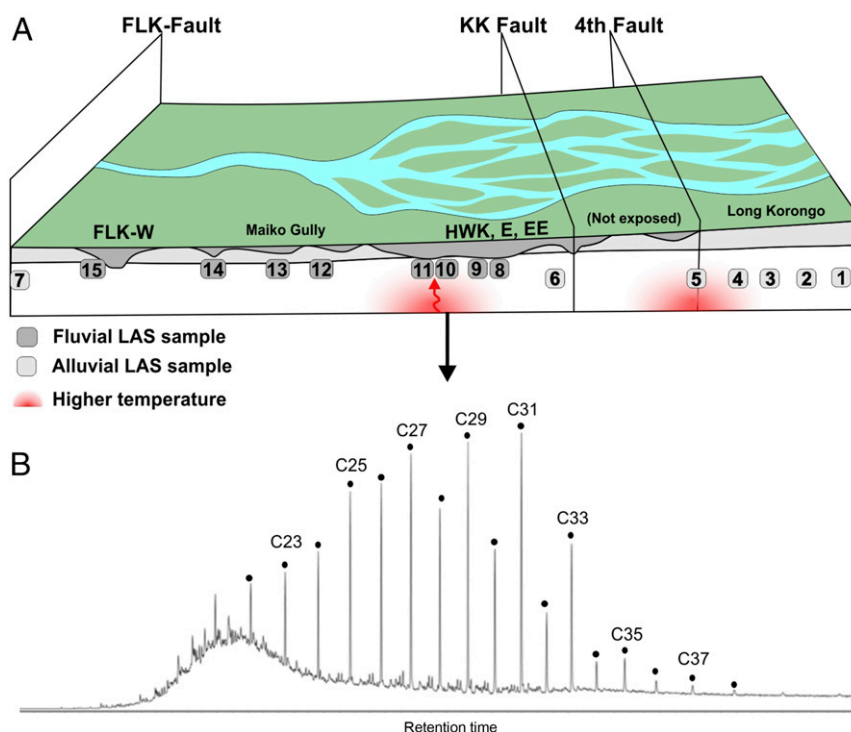


Fig. 5. Three-dimensional geomorphological reconstruction of the LAS unit between Long Korongo and FLK Fault during the dry season. (A) Three-dimensional reconstruction of the LAS landscape with the location of the hot spots according to the biomarker evidence. (B) Total ion chromatogram of one of LAS *n*-alkane fraction showing the coexistence of mature and immature organic matter within the sample.

within the lipids from FLK-W. Here, hominins concentrated large amounts of implements, notably Acheulian artifacts, in spatial association with faunal (including megafaunal) remains. Taphonomic evidence of exploitation of some of these resources by hominins has been reported (16).

The presence, in some samples, of biomarker assemblages typically associated with hyperthermophilic microbes suggests that parts of these streams or pools may have seen surface temperatures as high as 80 to 90 °C, although subsurface temperatures might have been higher. To cook, the only requirement is heat, and at such temperatures starches gelatinize, improving the accessibility of otherwise indigestible nutrients in roots and tubers that became more available with the progressive loss of canopy in Bed II. Cooking animal tissues in high-temperature waters would also have enhanced digestibility, palatability, and energy gain, reducing the exposure to foodborne pathogens (51) with the benefit of adding nutrients derived from the hot spring water (52). Carmody and Wrangham (53) pointed to the evolutionary significance of cooking in human evolution, and suggested that cooking might have begun with *Homo erectus* (53).

While nonopportunistic fire use is debated during early human evolution (53), hot springs may have offered *H. erectus* the opportunity to sustain the increased energetic costs of encephalization by providing an efficient way to thermally process the edible resources the wetland offered. The association of thermal springs in the proximity of archaeological sites documented here can also be found at other localities such as Koobi Fora (54) and Peninj (55), suggesting that the connection between hominin activities and thermal systems may not be fortuitous. Hominins may have sought these cooking opportunities, given the preference that chimpanzees exhibit for cooked food and their willingness to transport raw food in anticipation for future chances of cooking (56). Hydrothermal waters have traditionally been used for cooking in areas of Japan, New Zealand, the Azores, Thailand, India, and Iceland (57, 58).

Conclusions

Elucidating the possible complex interactions between early humans and their environment at Olduvai Gorge provides context for understanding early hominin evolution. Current interpretations of the Olduvai landscape 1.7 Ma rely largely on a broad-strokes approach to environmental reconstruction, while hominins may have experienced different and more dynamic local conditions. In the course of the present work, we encountered evidence via the composition of lipid biomarkers and their carbon isotopic ratios that the 1.7 My-old LAS sediments recorded a mosaic ecosystem, dominated by the presence of groundwater-fed rivers/channels and aquatic plants. Further, we observed few differences between the alluvial and fluvial landscapes, notably regarding water levels, suggesting that the hydrology of this area of the Gorge shifted toward a more seasonal environment but the vegetation and resources remained alike.

In the context of progressive aridification and expansion of savanna grasslands, the 1.7 My-old Olduvai Gorge paleolandscape evinced by our data was a groundwater-fed wetland with rivers partly sourced by hydrothermal waters and populated with patchy vegetation, comprising C3 aquatic plants, C4 grasses, and angiosperm shrublands potentially including edible plants such *Typha*, sedges, ferns, and palms. This type of patchy vegetation is seen in African wetlands today (35) and is highly dependent on water availability, temperature, and pH.

We also identified lipid biomarkers typical of contemporary hydrothermal features that are colonized by biofilm-forming microbes such as Aquificales and other thermophiles, with variations in community composition within the landscape. Geochemical evidence reveals a landscape with groundwater-fed habitats, in which hot springs and rivers partly sourced by thermal waters prompted intensive use by hominins.

The influence of hydrothermalism on early human evolution has not been addressed before. The accumulation of animal carcasses in the HWK and FLK-W sites suggest long-term, thorough

hominin use of the space near hydrothermal features (*SI Appendix, Table S1*), which likely attracted large herbivores as suggested by fecal biomarkers. Hot springs may have provided a convenient way to cook food that would have required minimal effort, which, at the same time, would have decreased digestibility-reducing components of starches. Cooking may, thus, have had a simple prefire stage during human evolution.

Materials and Methods

Sampling. Sample collection was carried out following the landscape paleogeography (downstream, southeast to northwest). In this way, collection of samples from the oldest to the most recent unit was facilitated. It is more common to find the alluvial unit overlying the LD in the East, whereas the river unit, somewhat more modern, is more abundant toward the west (Fig. 1). Accurate identification of the lower alluvial or the upper fluvial unit in the field is essential when taking samples for biomarker analysis, so as not to mix the two paleolandscapes. Since the sole identification of the LAS base is not an absolute isochronal criterion, the identification of the overlying subunit must be taken into account for a more detailed and precise isochronal surface.

Every effort was made to obtain the 15 samples at regular intervals, although the heterogeneous distribution of outcrops and the greater geological complexity in some areas has conditioned the distribution somewhat. All samples were taken in the LAS, in a position as close as possible to the base of the alluvial or river unit. Following these premises and criteria, samples 1 to 7 belong to the alluvial unit whereas samples 8 to 15 belong to the river unit (Fig. 1). Samples were collected from the basal 5 cm of the LAS using sterilized tools, wrapped in combusted aluminum foil, and stored in cloth bags.

Biomarker Extraction and Isolation. Sediment samples were freeze-dried and powdered prior to extraction. After addition of a recovery standard (1-pentadecanol), extraction was performed using and Accelerated Solvent Extractor (Dionex ASE 300 system) with dichloromethane (DCM) and methanol (MeOH) (9:1 vol/vol) using a method with three cycles of 15 min at 100 °C and 1,500 psi. The total lipid extract (TLE) was concentrated using a Turbovap with a gentle stream of N₂.

An aliquot of the TLE was derivatized via acid methanolysis (0.5 M HCl in methanol) diluted in H₂O and extracted with hexane:DCM (4:1 vol/vol). The derivatized extract was concentrated followed by separation into three fractions using a deactivated silica gel (2% H₂O total weight)-packed column by elution with hexane (F1), hexane:DCM (1:1) (F2), and DCM:MeOH (4:1). The polar fraction (F3) was then silylated using N,O-bis(trimethylsilyl) trifluoroacetamide.

Biomarker Analysis. Biomarkers were characterized by gas chromatography-mass spectrometry (GC-MS) with an Agilent 7890A series gas chromatograph interfaced with an Agilent 5977C mass selective detector. A 1-μL aliquot of apolar and derivatized extracts was injected in splitless mode onto a 60-m DB-

5MS fused-silica column (60-m × 0.25-mm internal diameter and film thickness of 0.25 μm). The GC oven temperature was programmed as follows: 60 °C injection and hold for 2 min, ramp at 6 °C min to 300 °C, followed by isothermal hold of 20 min. The transfer line, source, and quadrupole temperatures are set at 320 °C, 270 °C, and 150 °C, respectively, and the source was operated at 70 eV. Data were acquired, processed, and identified under the conditions described above. 1-Pentadecanol was used as a recovery standard and internal injection and response factors were calculated for the different lipid classes using representative standards (aiC₂₂, epiandrosterone, 1-nonadecanol, and 2-methyloctadecanoic acid methyl ester). Procedural blanks were run in order to monitor background interferences.

Compound-Specific Isotopic Analyses. Apolar fractions were subsequently analyzed to characterize their isotopic signatures using a Trace 1310 interfaced with a GC Isolink II connected to a Thermo MAT 253. A 1-μL aliquot was injected in splitless mode onto a 60-m DB5-MS column (60-m × 0.25-mm internal diameter and film thickness of 0.25 μm) before combustion over copper, nickel, and platinum wire with oxygen and helium at 1,000 °C. Isotopic values were normalized using a mixture of *n*-alkanes (C₁₆ to C₃₀) of known isotopic composition (mixture A5 of Arndt Schimmelmann). The SD for the instrument, based on replicate standard injection, was calculated to be below 0.4‰. All measurements were performed in duplicate. We only report here well-resolved analytes, corresponding to major compounds within the lipid classes.

Bulk Geochemical Analyses. For bulk analysis, about 3 g of sediment, previously freeze-dried and ground, was reacted with 1 N HCl to remove inorganic carbon then rinsed until reaching neutral pH. Analyses were carried on via elemental analysis-isotope ratio mass spectrometry for TOC, total nitrogen, and carbon isotopic composition of bulk organic matter using an ECS 4010 from Costech interfaced to a Thermo Finnigan Delta Plus XP.

Data Availability. All data pertaining to this study can be found in *SI Appendix*. GC-MS data have been deposited by Ainara Sistiaga at the Electronic Research Data Archive (ERDA) on 20 July 2020 (<https://erda.ku.dk/public/archives/947e13a6272ba9d74056e7010319486f/published-archive.html>).

ACKNOWLEDGMENTS. We thank the Tanzania Commission for Science and Technology, the Department of Antiquities, and the Ngorongoro Conservation Area Authority for field permits and support. Archaeological research at Olduvai Gorge is funded by the Spanish Government I+D project (HAR2017-82463-C4-1-P). Research at Massachusetts Institute of Technology was supported by a Marie Skłodowska Curie Global Fellowship (H2020-MSCA-IF-2016-750860) to A.S. and a grant (NNA13AA90A) from the NASA Astrobiology Institute to R.E.S. We are grateful to the crew at the Olduvai Paleoanthropology and Paleocology Project (TOPPP) archaeological project in Olduvai. We also thank X. Zhang and G. Izon for their assistance with compound-specific isotope analyses, and T. Evans for his assistance with the high-performance liquid chromatography quadrupole-time-of-flight mass spectrometric analyses.

1. L. S. B. Leakey, M. D. Leakey, *Olduvai Gorge, 1951-1961: Excavations in Beds I and II, 1960-1963*, (University Press, 1965).
2. C. R. Magill, G. M. Ashley, K. H. Freeman, Water, plants, and early human habitats in eastern Africa. *Proc. Natl. Acad. Sci. U.S.A.* **110**, 1175-1180 (2013).
3. C. R. Magill, G. M. Ashley, K. H. Freeman, Ecosystem variability and early human habitats in eastern Africa. *Proc. Natl. Acad. Sci. U.S.A.* **110**, 1167-1174 (2013).
4. D. E. Colcord et al., Aquatic biomarkers record Pleistocene environmental changes at Paleolake Olduvai, Tanzania. *Palaeogeogr. Palaeoclimatol. Palaeoecol.* **524**, 250-261 (2019).
5. D. M. Deocampo, P. A. Berry, E. J. Beverly, G. M. Ashley, R. E. Jarrett, Whole-rock geochemistry tracks precessional control of Pleistocene lake salinity at Olduvai Gorge, Tanzania: A record of authigenic clays. *Geology* **45**, 683-686 (2017).
6. P. B. deMenocal, Anthropology. Climate and human evolution. *Science* **331**, 540-542 (2011).
7. D. M. Deocampo, G. M. Ashley, Siliceous islands in a carbonate sea; Modern and Pleistocene spring-fed wetlands in Ngorongoro Crater and Oldupai Gorge, Tanzania. *J. Sediment. Res.* **69**, 974-979 (1999).
8. G. M. Ashley, M. Dominguez-Rodrigo, H. T. Bunn, A. Z. P. Mabulla, E. Baquedano, Sedimentary geology and human origins: A fresh look at Olduvai Gorge, Tanzania. *J. Sediment. Res.* **80**, 703-709 (2010).
9. H. Arráziz et al., The FLK Zinj paleolandscape: Reconstruction of a 1.84Ma wooded habitat in the FLK Zinj-AMK-PTK-DS archaeological complex, middle bed I (Olduvai Gorge, Tanzania). *Palaeogeogr. Palaeoclimatol. Palaeoecol.* **488**, 9-20 (2017).
10. G. M. Ashley, J. C. Taktikos, R. Bernhart Owen, Hominin use of springs and wetlands: Paleoclimate and archaeological records from Olduvai Gorge (~1.79-1.74 Ma). *Palaeogeogr. Palaeoclimatol. Palaeoecol.* **272**, 1-16 (2009).
11. R. L. Hay, *Geology of the Olduvai Gorge: A Study of Sedimentation in a Semiarid Basin*, (University of California Press, 1976).
12. D. Uribelarra et al., A geoarchaeological reassessment of the co-occurrence of the oldest Acheulean and Oldowan in a fluvial ecotone from lower middle Bed II (1.7Ma) at Olduvai Gorge (Tanzania). *Quat. Int.* **526**, 39-48 (2019).
13. D. Uribelarra et al., A reconstruction of the paleolandscape during the earliest Acheulean of FLK West: The co-existence of Oldowan and Acheulean industries during lowermost bed II (Olduvai Gorge, Tanzania). *Palaeogeogr. Palaeoclimatol. Palaeoecol.* **488**, 50-58 (2017).
14. T. Proffitt, Is there a developed Oldowan A at Olduvai Gorge? A diachronic analysis of the Oldowan in bed I and lower-middle bed II at Olduvai Gorge, Tanzania. *J. Hum. Evol.* **120**, 92-113 (2018).
15. F. Diez-Martín et al., The origin of the Acheulean: The 1.7 million-year-old site of FLK West, Olduvai Gorge (Tanzania). *Sci. Rep.* **5**, 17839 (2015).
16. J. Yravedra et al., FLK West (lower bed II, Olduvai Gorge, Tanzania): A new early Acheulean site with evidence for human exploitation of fauna. *Boreas* **46**, 816-830 (2017).
17. T. E. Cerling, R. L. Hay, An isotopic study of paleosol carbonates from Olduvai Gorge. *Quat. Res.* **25**, 63-78 (1986).
18. M. H. Trauth, M. A. Maslin, A. Deino, M. R. Strecker, Late Cenozoic moisture history of East Africa. *Science* **309**, 2051-2053 (2005).
19. R. T. Bush, F. A. McInerney, Leaf wax *n*-alkane distributions in and across modern plants: Implications for paleoecology and chemotaxonomy. *Geochim. Cosmochim. Acta* **117**, 161-179 (2013).
20. A. F. Diefendorf, E. J. Freimuth, Extracting the most from terrestrial plant-derived *n*-alkyl lipids and their carbon isotopes from the sedimentary record: A review. *Org. Geochem.* **103**, 1-21 (2017).
21. K. E. Peters, C. C. Walters, J. M. Moldovan, *The Biomarker Guide*, (Cambridge University Press, 2004).

22. K. J. Ficken, B. Li, D. L. Swain, G. Eglinton, An n-alkane proxy for the sedimentary input of submerged/float freshwater aquatic macrophytes. *Org. Geochem.* **31**, 745–749 (2000).
23. C. R. Magill, G. M. Ashley, M. Domínguez-Rodrigo, K. H. Freeman, Dietary options and behavior suggested by plant biomarker evidence in an early human habitat. *Proc. Natl. Acad. Sci. U.S.A.* **113**, 2874–2879 (2016).
24. B. D. A. Naafs, G. N. Inglis, J. Blewett, E. L. McClymont, The potential of biomarker proxies to trace climate, vegetation, and biogeochemical processes in peat: A review. *Glob. Planet. Change* **179**, 57–79 (2019).
25. J. E. Nichols, Y. Huang, C23–C31 n-alkan-2-ones are biomarkers for the genus *Sphagnum* in freshwater peatlands. *Org. Geochem.* **38**, 1972–1976 (2007).
26. M. K. Bamford, R. M. Albert, D. Cabanes, Plio-Pleistocene macroplant fossil remains and phytoliths from Lowermost Bed II in the eastern palaeolake margin of Olduvai Gorge, Tanzania. *Quat. Int.* **148**, 95–112 (2006).
27. R. D. Pancost *et al.*, Composition and implications of diverse lipids in New Zealand Geothermal sinters. *Geobiology* **4**, 71–92 (2006).
28. L. L. Jahnke *et al.*, Signature lipids and stable carbon isotope analyses of Octopus Spring hyperthermophilic communities compared with those of Aquificales representatives. *Appl. Environ. Microbiol.* **67**, 5179–5189 (2001).
29. F. Schubotz *et al.*, Spatial and temporal variability of biomarkers and microbial diversity reveal metabolic and community flexibility in streamer biofilm communities in the Lower Geyser basin, Yellowstone national park. *Geobiology* **11**, 549–569 (2013).
30. S. A. Newman *et al.*, Lipid biomarker record of the serpentinite-hosted ecosystem of the samail ophiolite, Oman and implications for the search for Biosignatures on Mars. *Astrobiology* **20**, 830–845 (2020).
31. D. R. Meyer-Dombard *et al.*, Hydrothermal ecotones and streamer biofilm communities in the Lower Geyser basin, Yellowstone national park. *Environ. Microbiol.* **13**, 2216–2231 (2011).
32. A. S. Bradley, H. Fredricks, K.-U. Hinrichs, R. E. Summons, Structural diversity of diether lipids in carbonate chimneys at the Lost City Hydrothermal Field. *Org. Geochem.* **40**, 1169–1178 (2009).
33. O. Bertrand *et al.*, Recent vegetation history from a swampy environment to a pond based on macromolecular organic matter (lignin and fatty acids) and pollen sedimentary records. *Org. Geochem.* **64**, 47–57 (2013).
34. Y. Chikaraishi, H. Naraoka, Compound-specific $\delta^{13}\text{C}$ analyses of n-alkanes extracted from terrestrial and aquatic plants. *Phytochemistry* **63**, 361–371 (2003).
35. R. B. Owen, R. W. Renaut, V. C. Hoyer, G. M. Ashley, A. M. Muasya, Swamps, springs and diatoms: Wetlands of the semi-arid Bogoria-Baringo Rift, Kenya. *Hydrobiologia* **518**, 59–78 (2004).
36. C. B. Osmond, N. Valaane, S. M. Haslam, P. Uotila, Z. Roksandic, Comparisons of $\delta^{13}\text{C}$ values in leaves of aquatic macrophytes from different habitats in Britain and Finland; some implications for photosynthetic processes in aquatic plants. *Oecologia* **50**, 117–124 (1981).
37. V. Grossi *et al.*, Mono- and dialkyl glycerol ether lipids in anaerobic bacteria: Biosynthetic insights from the mesophilic sulfate reducer *Desulfatibacillum alkenivorans* PF2803T. *Appl. Environ. Microbiol.* **81**, 3157–3168 (2015).
38. M. T. Hernandez-Sanchez, W. B. Homoky, R. D. Pancost, Occurrence of 1-O-monoalkyl glycerol ether lipids in ocean waters and sediments. *Org. Geochem.* **66**, 1–13 (2014).
39. Y. Wang, Y. Xu, Distribution and source of 1-O-monoalkyl glycerol ethers in the yellow river and Bohai Sea. *Org. Geochem.* **91**, 81–88 (2016).
40. H. Yang, F. Zheng, W. Xiao, S. Xie, Distinct distribution revealing multiple bacterial sources for 1-O-monoalkyl glycerol ethers in terrestrial and lake environments. *Sci. China Earth Sci.* **58**, 1005–1017 (2015).
41. R. Huber *et al.*, *Thermocrinis ruber* gen. nov., sp. nov., A pink-filament-forming hyperthermophilic bacterium isolated from Yellowstone national park. *Appl. Environ. Microbiol.* **64**, 3576–3583 (1998).
42. R. Huber *et al.*, *Aquifex pyrophilus* gen. nov. sp. nov., represents a novel group of marine hyperthermophilic hydrogen-oxidizing bacteria. *Syst. Appl. Microbiol.* **15**, 340–351 (1992).
43. K. Prost, J. J. Birk, E. Lehnendorff, R. Gerlach, W. Amelung, Steroid biomarkers revisited—Improved source identification of faecal remains in archaeological soil material. *PLoS One* **12**, e0164882 (2017).
44. R. D. Pancost *et al.*, Archaeol as a methanogen biomarker in ombrotrophic bogs. *Org. Geochem.* **42**, 1279–1287 (2011).
45. A. B. Banta, J. H. Wei, P. V. Welander, A distinct pathway for tetrahymanol synthesis in bacteria. *Proc. Natl. Acad. Sci. U.S.A.* **112**, 13478–13483 (2015).
46. R. N. Leif, B. R. T. Simoneit, Ketones in hydrothermal petroleum and sediment extracts from Guaymas Basin, Gulf of California. *Org. Geochem.* **23**, 889–904 (1995).
47. M. Reinhardt *et al.*, Organic signatures in Pleistocene cherts from Lake Magadi (Kenya), analogs for early Earth hydrothermal deposits. *Biogeosciences Discuss.*, <https://doi.org/10.5194/bg-2018-513> (2019).
48. D. M. Martín-Perea *et al.*, Mineral assemblages and low energy sedimentary processes in the FLK-Zinj, DS, PTK and AMK complex palaeolandscape (Olduvai Gorge, Tanzania). *Quat. Int.* **526**, 15–25 (2019).
49. G. Bailey, R. Charles, N. Winder, “Tectonics, volcanism, landscape structure and human evolution in the African Rift” in *Human Ecodynamics: Symposia of the Association for Environmental Archaeology*, G. Bailey, R. Charles, N. Winder, Eds. (Oxbow Books, 2000), p. 15.
50. H. Arraiz Rodríguez, “Reconstrucción de la paleovegetación y uso de útiles líticos en el yacimiento de homínidos de la garganta de Olduvai (Tanzania) mediante el uso de microfósiles vegetales,” PhD thesis, Universidad Complutense de Madrid, Madrid (2016).
51. A. R. Smith, R. N. Carmody, R. J. Dutton, R. W. Wrangham, The significance of cooking for early hominin scavenging. *J. Hum. Evol.* **84**, 62–70 (2015).
52. R. N. Carmody, G. S. Weintraub, R. W. Wrangham, Energetic consequences of thermal and nonthermal food processing. *Proc. Natl. Acad. Sci. U.S.A.* **108**, 19199–19203 (2011).
53. R. N. Carmody, R. W. Wrangham, The energetic significance of cooking. *J. Hum. Evol.* **57**, 379–391 (2009).
54. R. W. Renaut, K. K. Morley, B. Jones, “Fossil hot-spring travertine in the Turkana basin, northern Kenya: Structure, facies, and genesis” in *Sedimentation in Continental Rifts*, R. W. Renaut, G. M. Ashley, Eds. (Society for Sedimentary Geology, 2002), pp. 123–141.
55. M. Domínguez-Rodrigo, L. Alcalá, L. Luque, *Peninj: A Research Project on Human Origins 1995–2005*, (Oxbow Books, 2009).
56. F. Warneken, A. G. Rosati, Cognitive capacities for cooking in chimpanzees. *Proc. Biol. Sci.* **282**, 20150229 (2015).
57. G. Neilson, G. Bignall, D. Bradshaw, “Whakarewareware a living thermal village—Rotorua, New Zealand” in *Proceedings of the World Geothermal Congress*, (International Geothermal Association, 2010), pp. 1–7.
58. R. Cataldi, S. F. Hodgson, J. W. Lund, *Stories from a Heated Earth: Our Geothermal Heritage*, (Nicholson, 1999).